

Spectroscopy and Photophysics of a Highly Nonplanar Expanded Porphyrin: 4,9,13,18,22,27-Hexaethyl-5,8,14,17,23,26-hexamethyl-2,11,20-triphenylrosarin

B. Lament,^[a] J. Dobkowski,^[a] J. L. Sessler,^[b] S. J. Weghorn,^[b] and J. Waluk*^[a]

Abstract: The structure and spectra of neutral and protonated forms of rosarin, a nonaromatic hexapyrrolic expanded porphyrin bearing three phenyl and twelve alkyl substituents, were studied by means of stationary and picosecond time-resolved spectral techniques and by molecular mechanics and quantum-chemical calculations. The photophysics of the lowest excited singlet state is dominated by rapid internal conversion to the ground state. No fluorescence could be detected. This behavior was

attributed to the nonplanarity and conformational flexibility of the molecule. Triplet formation efficiency is negligible as long as the solvent does not contain heavy atoms. In the presence of iodine, a significant fraction of the excited-singlet-state population was found to cross over to the triplet state. The absorption

spectral pattern consists of a weak transition in the red spectral region, well separated from the strong bands observed at higher energy. Analysis of the calculations reveals why only one transition is predicted in the low-energy region. In contrast to porphyrin, whose spectra can be understood in terms of a four orbital model, the interpretation of the spectral features of rosarin requires six orbitals: the three highest occupied and the three lowest unoccupied ones.

Keywords: electronic structure • expanded porphyrins • porphyrinogens • protonations • rosarin

Introduction

Synthetic studies aimed at producing new porphyrin derivatives with novel properties remain of considerable current interest owing to the many possible applications wherein such systems might find a useful role. Recent years have witnessed successful syntheses of a large number of pyrrole-containing macrocycles, including such diverse entities as isomeric, “contracted”, and “expanded” porphyrins.^[1] The last class of compounds, in particular, turns out to be one of particular importance especially with regard to various biomedical applications, such as photodynamic therapy,^[2] radiation sensitization,^[3] and anion-complexing agents.^[1] Expanded porphyrins possessing up to ten pyrrole units have been reported.^[4] Depending on the specifics of structure and the number of pyrroles contained within the framework, the molecules themselves are seen to adopt geometries and topologies that range from completely planar to complex and

Möbius-like. It is natural to expect that such molecular characteristics as the degree of planarity, π -electron conjugation, and aromaticity as well as the generalized chemical characteristics will be strongly interdependent. Especially pronounced should be the correlation between the spectral and photophysical properties. It is well known, for instance, that introducing strain into the porphyrin skeleton leads to a decrease in the radiative properties and to an enhancement in the rates of radiationless depopulation of the associated excited states.^[5]

In this work, we present spectral studies of 4,9,13,18,22,27-hexaethyl-5,8,14,17,23,26-hexamethyl-2,11,20-triphenylrosarin (**1**, Figure 1). This hexapyrrolic macrocycle can be represented as a nonaromatic, conjugated 24 π -electron chromophore.^[6] An X-ray diffraction structure of the chloride salt of the triply protonated form of **1** reveals a nonplanar structure in the solid state. In this paper we show that the nonplanarity, which results in considerable flexibility in the molecular skeleton, has profound photophysical consequences. For instance, very rapid radiationless deactivation to the ground state is detected for both the protonated and neutral forms of **1**. Further, the lowest excited state depopulation is dominated by $S_0 \leftarrow S_1$ internal conversion: no fluorescence or crossing over to the triplet state can be observed. The latter, however, can be induced by an external heavy atom effect.

The experimental results are combined with calculations of molecular geometry and electronic structure. The electronic absorption patterns are quite well reproduced by these

[a] Prof. Dr. J. Waluk, B. Lament, Dr. J. Dobkowski
Institute of Physical Chemistry, Polish Academy of Sciences
Kasprzaka 44, PL-01-224 Warsaw (Poland)
Fax: (+48) 391-20238
E-mail: waluk@alfa.ichf.edu.pl

[b] Prof. J. L. Sessler, Dr. S. J. Weghorn
Department of Chemistry and Biochemistry
University of Texas at Austin, Texas 78712 (USA)
Fax: (+1) 512-471-7550
E-mail: sessler@mail.utexas.edu

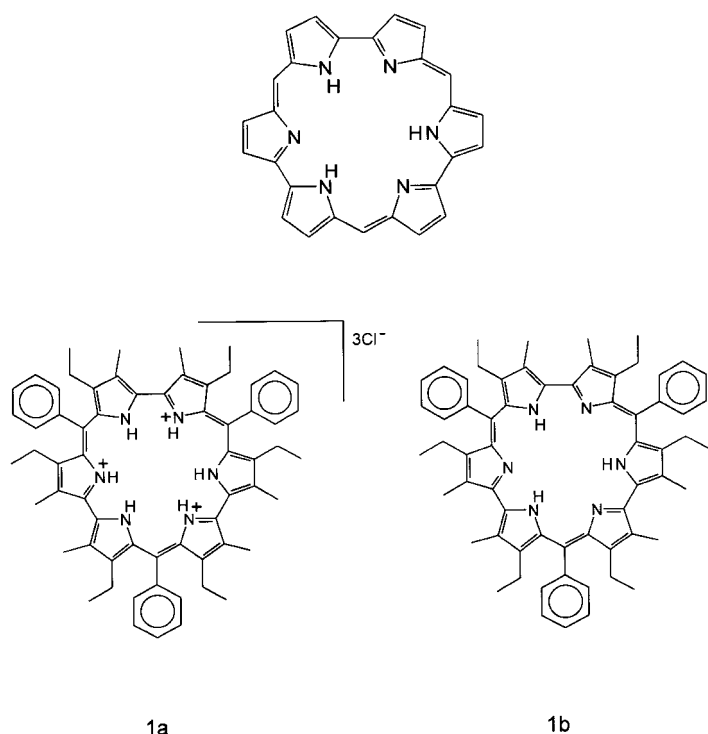


Figure 1. Top: parent rosarin. Bottom: triply protonated form (**1a**); neutral form (**1b**).

calculations. However, these same theoretical analyses show that the standard model, which requires four frontier orbitals in the explanation of the spectral properties of porphyrin-related compounds, cannot be applied in the present case. Indeed, at least six molecular orbitals should be taken into account for rosarin in order to properly predict its absorption characteristics.

Abstract in Polish: Zbadano strukturę i widma obojętnej i protonowanych form rozaryny – niearomatycznej heksapirowej rozszerzonej porfiryny, podstawionej trzema grupami fenyłowymi i dwunastoma grupami alkilowymi. Zastosowano techniki stacjonarnej i czasowo-rozdzielczej pikosekundowej spektroskopii oraz obliczenia metodami mechaniki molekularnej i chemii kwantowej. Fotofizyka najniższego singletowego stanu wzbudzonego jest zdominowana przez szybką konwersję wewnętrzną do stanu podstawowego. Żadna z form rozaryny nie wykazuje fluorescencji, co zostało przypisane nieplanarności i konformacyjnej giętkości cząsteczki. Wydajność tworzenia stanu trypletowego jest zaniedbywalna dopóty, dopóki rozpuszczalnik nie zawiera ciężkiego atomu. W obecności jodu, znaczna część wzbudzonej populacji przechodzi do stanu trypletowego. Absorpcja rozaryny wykazuje słabe przejście w czerwonym obszarze widma, dobrze oddzielone od dwóch silnych pasm obserwowanych w zakresie wyższych energii. Analiza wyników obliczeń pozwala zrozumieć dlaczego w niskoenergetycznym obszarze przewidywane jest tylko jedno przejście. W przeciwieństwie do porfiryny, której widma dobrze opisuje model uwzględniający cztery orbitale molekularne, prawidłowa interpretacja widm rozaryny wymaga wzięcia pod uwagę sześciu orbitali.

Experimental Section and Computational Details

The synthesis and purification of **1** was performed as described earlier.^[6] Spectral grade solvents were used in all measurements. Absorption spectra were recorded on a Shimadzu UV3100 spectrophotometer. Attempts to register fluorescence spectra were done by using either an Edinburgh Instruments FS900 steady state spectrometer or a Jasný spectrofluorimeter^[7] equipped with a home-built near-IR monochromator and a Hamamatsu R632 photomultiplier, which extended the detection range to 1100 nm. A home-built picosecond transient absorption instrument^[8] with a parametric oscillator (EKSPLA) was used for the time-resolved studies of spectral bleaching and ground-state recovery. For experiments involving heavy atom effects, a Jasný nanosecond transient-absorption spectrometer^[9] was also used. Stationary absorption was measured before and after picosecond experiments, to ensure that no decomposition of the sample occurred.

Ground-state geometry optimization studies were performed by means of either molecular mechanics (MMX, PCMODEL program^[10]) or MM + ^[11] (Hyperchem package) force fields or semiempirical quantum chemistry methods (AM1^[12] and PM3,^[13] as implemented in Hyperchem). Excited-state parameters (transition energies, oscillator strengths) were computed by use of our own code for calculations with the INDO/S method,^[14] 460 lowest singly excited configurations were taken into account in the CI (configuration interaction) procedure.

Results and Discussion

Absorption spectra of **1** vary from solvent to solvent, as a complicated function of its polarity and, most importantly, its acidity. Qualitative acid–base titration studies revealed the presence of four different forms. These, we attribute to the neutral, singly, doubly, and triply protonated forms of rosarin **1**, respectively (Table 1). Figure 2 presents the spectra which,

Table 1. Absorption maxima (in wavenumbers) corresponding to various protonated forms.

Trication ^[a] (BH_3^{3+} , 1a)	Doubly protonated form ^[a] (BH_2^{2+})	Singly protonated form ^[b] (BH^+)	Neutral molecule ^[c] (B , 1b)
12300	13600	12300	15600
13900			
15550			
18320 ^[d]	20150 ^[d]	21150 ^[d]	20800 ^[d]
19700 sh			
23500	26200		~28500
30200		31400	
37500	36700	36900	~33000

[a] Methanol solution with perchloric acid. [b] Methanol. [c] Methanol with triethylamine. [d] The strongest transition.

based on titration experiments, we assign to the triply protonated structure (**1a**) and to the neutral form (**1b**). It was difficult to obtain the separate spectra of the intermediate forms. For instance, upon adding acid to solutions of the free-base (i.e., neutral) or monoprotonated derivatives, spectral features belonging to the doubly protonated species, with an absorption maximum at around 20150 cm^{-1} , appear practically simultaneously with those that are ascribable to the triply protonated form, a species characterized by an absorption maximum around 18320 cm^{-1} (see Figure 3). This finding leads us to infer that the pK_a values associated with the second and third protonation steps are very close. In many cases, we observed absorption spectra that revealed bands belonging to more than one species. The intensity ratios of these bands

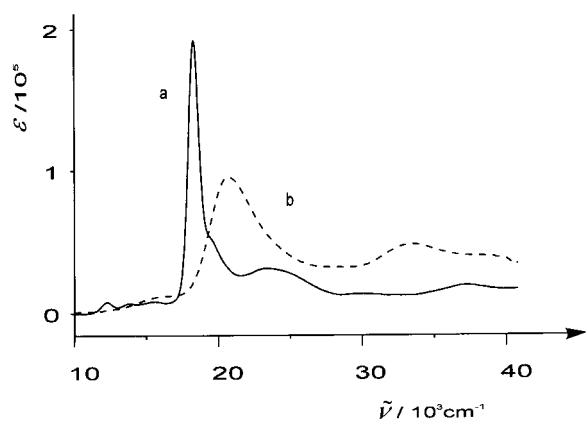


Figure 2. Absorption spectra of the triply protonated form of **1** (curve a, recorded in acetonitrile with 0.7 M perchloric acid) and of the neutral structure (curve b, solution in methanol with 0.23 M triethylamine).

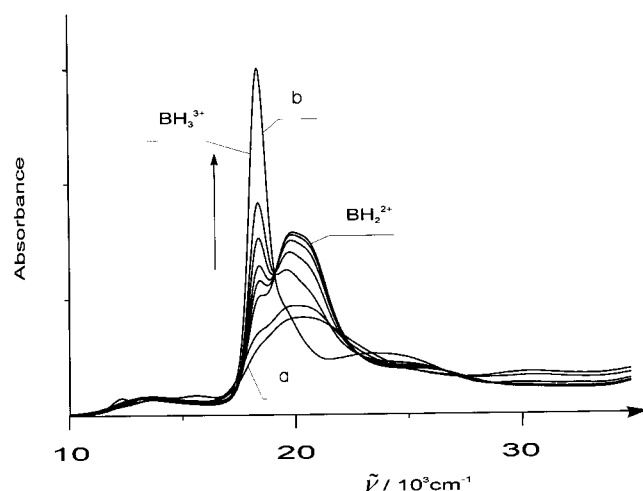


Figure 3. Spectral changes accompanying titration of a methanolic solution of **1** with sulfuric acid. Spectrum a) corresponds to pure methanol, spectrum b) to a 0.1 M concentration of the acid.

were found to change not only as a function of different solvents, but were also found to be, on occasion, quite different for different batches of the same solvent; they showed, in particular, extreme sensitivity to the presence of protic impurities. Specific effects, most probably involving hydrogen-bonding interactions with the solvent or counteranion binding, could also influence the protolytic equilibria.

The effect of solvent and putative impurities was most dramatic in the case of alcoholic solutions. Figure 4 shows the changes in the absorption spectra that accrue when methanol is added to a solution of rosarin in *n*-butyl alcohol. In pure *n*-butyl alcohol, triply and doubly protonated species dominate. As the concentration of methanol increases, the spectra evolve towards those of singly protonated species. This result is somewhat unexpected, given that butanol is more basic than methanol. Complementary, but different behavior is observed when slightly acidified solutions of rosarin in methanol are titrated with *n*-propyl alcohol. In this instance, the starting solutions contain **1a** and the corresponding di- and monocationic forms. However, the triply protonated species (**1a**) was found to disappear as the more basic alcohol (*n*-propyl alcohol) was added. Interestingly, the reverse titration, that is,

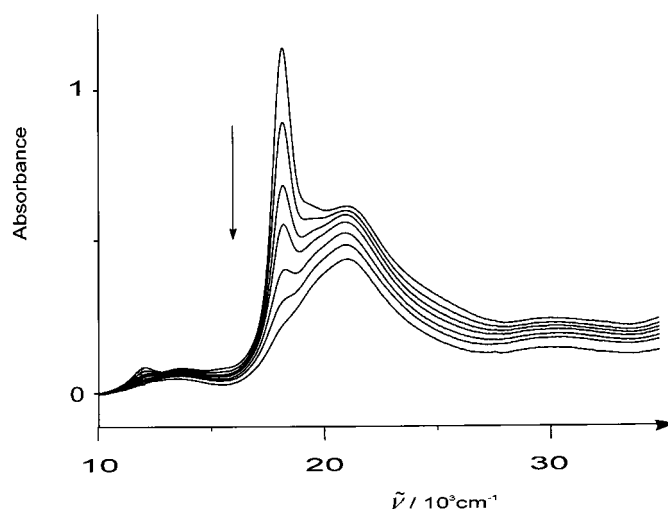


Figure 4. Changes in absorption spectra of an *n*-butyl alcohol solution of **1** observed upon addition of methanol. Methanol concentrations used varied from 0 to 10.6 M. The arrow shows the spectral evolution that occurs as increased amounts of methanol are added.

adding methanol to an *n*-propyl alcohol solution, did not produce any changes in the spectrum; in this instance, the spectral features always corresponded to those of the monocation.

It must be stressed that while our spectral assignments for the triply and doubly protonated species seem secure, the situation with the monocation and, to some extent, with neutral species is less clear. Our assignment of the latter is based on the spectra obtained upon addition of various bases to the solution. Thus, we cannot completely exclude the presence of deprotonated (i.e., pyrrole anion) structures. Likewise, the monocation was assigned to the spectrum that is intermediate between that thought to correspond to the doubly protonated species and that observed in basic solutions (i.e., that assigned to the free base). One should note also that several tautomeric forms of the monoprotonated structure are possible. Actually, we have observed very slow changes in the absorption spectra of methanolic solutions that we believe contain (predominantly) the monocation, a finding that is consistent with either tautomerization or isomerization, or perhaps a combination of both. In particular, it was noted that after about two days, the lowest absorption band was shifted to the blue by about 1200 cm^{-1} . Titration of the resulting solution by acids and bases restored the spectra of **1a** and **1b**, respectively. On this basis, we rule out the idea that these slow spectral changes are due to chemical decomposition. We also checked that they were not caused by sample aggregation or as the result of water being absorbed into the solution. Still, it is important to appreciate that further study, possibly with sterically encumbered derivatives, will be needed to sort out the exact details of the underlying chemistry.

Doubts about the assignments notwithstanding, it is clear that the spectral patterns observed for the various protonated rosarins are quite similar. For both **1a** and **1b**, as well as for other species, the strongest absorption band is preceded at lower energy by at least one weaker transition (Figure 2). In the case of **1b**, one broad peak centered at 15600 cm^{-1} was observed. For **1a**, three peaks are seen, with the maximum of the first one located at 12300 cm^{-1} . The equal spacing of the

peaks, about 1600 cm^{-1} , leads us to conclude that they represent progressions of the same electronic transition. At first glance, the spectra look rather similar to those of porphyrinoids. However, as discussed later, the analogy is rather fortuitous.

The values of the radiative constants of the lowest excited singlet state in **1a** and **1b** were estimated from an integration of the absorption in the region of the lowest electronic transition.^[15] This procedure yielded practically the same value of $3 \times 10^7\text{ s}^{-1}$ for **1a** and **1b**. Although the value of the corresponding oscillator strength (0.13) is not small, no fluorescence from either form could be detected, even at liquid nitrogen temperature. Thus, a very efficient nonradiative S_1 depopulation channel must be effective. In order to determine its nature, we have performed time-resolved picosecond studies, analyzing the time profile of the spectral transients. Figure 5 presents the results obtained for the

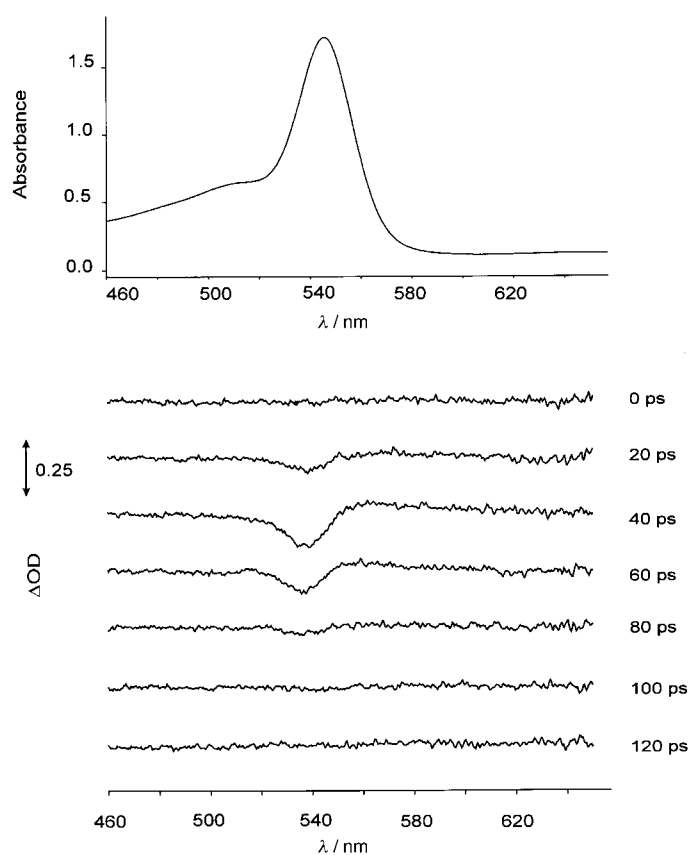


Figure 5. Top: stationary absorption of a sample of **1a** in acetonitrile acidified with perchloric acid. Bottom: transient signals observed at various delays from the edge of the exciting pulse.

protonated form **1a**. A negative absorption is observed at the wavelength corresponding to the stationary absorption maximum. It is thought to arise from ground state bleaching. Somewhat to the red, a positive absorption is observed that starts at the same moment as the bleaching. This feature is assigned to a $S_n \leftarrow S_1$ transition, that is, an absorption from the lowest excited singlet to a higher excited singlet state. Both transients decay with the same rate, disappearing very rapidly, faster than the time resolution of our instrument, which is about 30 ps. Indeed, after few tens of picoseconds, a total recovery of the ground state is achieved.

Similar results were observed for the neutral species **1b** as well as for the structure which we assign to the doubly protonated form. Thus, the decay of the lowest excited singlet state in **1** is dominated by an $S_0 \leftarrow S_1$ internal conversion process, the rate for which is apparently faster than 10^{11} s^{-1} . Since the values of radiative rate constants are about $3 \times 10^7\text{ s}^{-1}$, the upper limit for the fluorescence quantum yield is 3×10^{-4} , which is below the sensitivity of our instrument in the red spectral range. This explains why no fluorescence could be detected.

The large values for the internal conversion rates observed for the various forms of **1** cannot be explained solely by the low energy of S_1 and, thus, by the small S_0-S_1 energy gap. Indeed, we have detected fluorescence in expanded porphyrins that absorb further to the red than rosarin, namely 2,7,14,19-tetra-*tert*-butyl[22]porphyrin-(0.4.0.4) and 2,7,16,21-tetra-*tert*-butyl[26]porphyrin-(0.6.0.6).^[16] Based on this last experimental observation, we propose that another factor must be responsible for the large radiationless depopulation rate. Most probably, the origin of the rapid IC lies in the conformational flexibility of the molecule. The geometry in S_1 may be quite different from that of the ground state, which provides favorable conditions for fast radiationless deactivation. We have recently postulated that such a situation pertains in the case of dibenzoporphycenes;^[17] other examples involving porphyrin derivatives are also known.^[5] One should note that the lack of fluorescence at low temperatures implies that the radiationless process is either barrierless or does not require a significant activation energy.

Another possible mechanism of the efficient $S_0 \leftarrow S_1$ internal conversion could involve fast exchange of the internal protons between nitrogen atoms, a process we have discussed for dibenzoporphycenes.^[17] However, such proton shift is not possible in the triply protonated species, for which we still observe radiationless depopulation as efficient as in other forms. Therefore, we conclude that the main reason for the rapid S_1 deactivation is the nonplanar structure, which is characteristic for all stages of protonation.

Experimental confirmation of the nonplanarity of **1** comes from the X-ray analysis of the trishydrochloride salt. A strongly deformed, nonplanar structure is revealed.^[6] While this fact is illustrative, it still provides only one data point. We thus looked more closely at the reasons for nonplanarity by performing calculations for the parent structure of both unsubstituted rosarin and several substituted derivatives.

Molecular mechanics and semiempirical quantum-mechanical calculations predict that the parent rosarin should be planar, both in its fully protonated and neutral forms. However, a substitution by phenyl groups on the three "meso-like" carbon atoms leads to a distortion from planarity. A much larger distortion is predicted for the still unknown 4,9,13,18,22,27-hexaethyl-5,8,14,17,23,26-hexamethyl derivative. When both phenyl and alkyl substituents are introduced, the nonplanarity of the putative product becomes quite pronounced. Various conformers are predicted, some of them approaching "inverted" structures, in which at least one pyrrole ring is twisted in such a way that the NH group lies on the outside of the inner cavity. Similar inverted structures, initially discovered for tetraphenylporphyrin,^[18] have been recently

described in the case of *meso*-aryl-substituted sapphyrins,^[19] another well-known class of expanded porphyrins.^[1]

Various expanded porphyrins are known to bind anions.^[1] We therefore tried to make rosarin more rigid by the formation of complexes with fluoride or phosphate anions. However, the addition of either sodium fluoride or phosphoric acid to solutions of **1** did not produce measurable changes in the fast decay pattern. On the other hand, for the triply protonated form **1a** the recovery time of the ground-state bleaching became much longer upon addition of potassium iodide or *tert*-butyl iodide (Figures 6 and 7). This

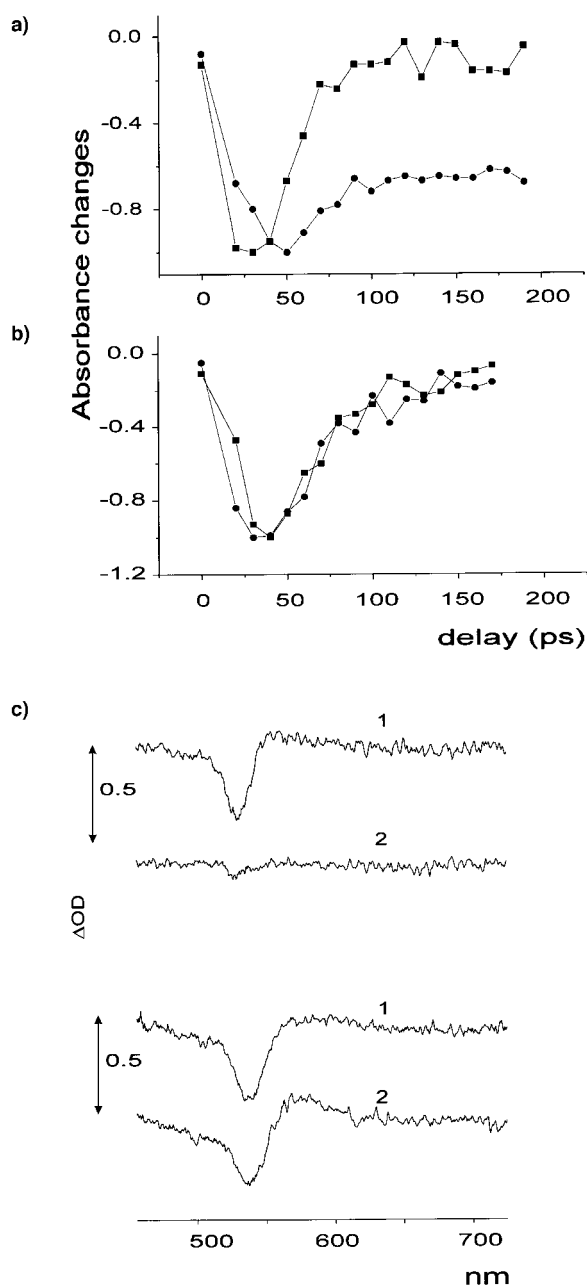


Figure 6. Time profiles of the bleaching signals obtained by integrating the transient spectra at each delay: a) acidified methanol; b) methanol. Circles: solutions containing *tert*-butyl iodide (2.5×10^{-3} M); squares: solutions without *tert*-butyl iodide. c) transient signals observed at 30 ps (1) and 100 ps (2) delays from the excitation for **1a** in acidified methanol. Top: solution without potassium iodide. Bottom: with potassium iodide (4.5×10^{-3} M).

was attributed to the efficient population of the triplet state in the presence of external heavy atoms. From the amplitude ratio of the rapid and slow recovery signals (Figure 6a), a triplet formation efficiency of 0.70 ± 0.20 could be estimated. It should be noted that the heavy atom enhanced $T_1 \leftarrow S_1$ intersystem-crossing rate must be very high ($>10^{11} \text{ s}^{-1}$) in order to effectively compete with the fast $S_0 \leftarrow S_1$ internal conversion. Heavy-atom-enhanced $S_0 \leftarrow T_1$ intersystem crossing is also very rapid, as evidenced by practically the same kinetic curves in the presence and absence of oxygen (Figure 7). Since the triplet lifetime is only a few nanoseconds,

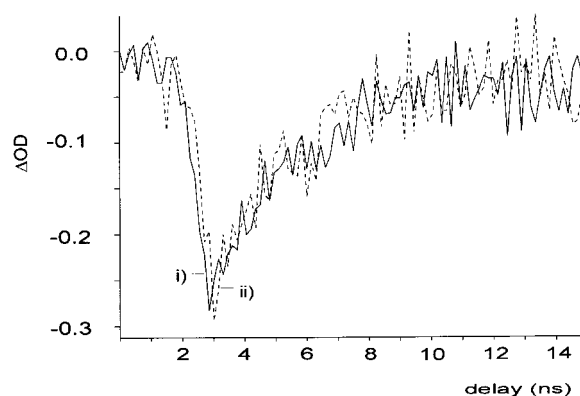


Figure 7. Time profiles of the bleaching signals of **1a** in acidified methanol containing *tert*-butyl iodide (2.5×10^{-3} M). The signals were obtained for both i) aerated and ii) deaerated solutions by monitoring at 555 nm.

diffusion-controlled oxygen quenching is not effective. In turn, the fact that triplet population is induced in **1a**, but not in **1b** (cf. Figures 6a and 6b) may indicate that the excited singlet state lifetime of the latter is shorter.

Excited-state energies, calculated for both the neutral and triply protonated parent rosarin, are presented in Table 2. The predicted pattern for the excited states is different from that of porphyrin. The reason lies in the high symmetry of parent **1** and the resulting ordering of molecular orbitals (Figure 8). In porphyrin and its derivatives, the excited-state properties are quite accurately described with the so-called “four-orbital model”.^[20] This model requires the use of only the two highest occupied and two lowest unoccupied π molecular orbitals, all of which are well separated in energy from the other orbitals. This “four-orbital model” approach also works quite well for porphycene, a porphyrin isomer.^[17] In rosarin, by contrast, more orbitals contribute to the lowest excited states. As a consequence, the minimal basis set now involves the three highest occupied and three lowest unoccupied orbitals, that is, nine singly excited configurations. Two pairs of these frontier orbitals are degenerate, due to the threefold symmetry of the molecule. This high symmetry also implies that many transitions have zero oscillator strengths and that the predicted number of allowed transitions will be quite small for a molecule of this size.

In order to find out how the spectrum evolves in the substituted, nonplanar structure, we used a simplified procedure. The large number and size of substituents did not allow the calculations of excited states of **1a** and **1b**. Therefore, after optimizing **1a** and **1b** by the use of molecular mechanics,

Table 2. Results of INDO/S calculations of transition energies, oscillator (Osc) strengths, and symmetries (Symm) for the parent, unsubstituted rosarin. An idealized planar, C_{3h} geometry was assumed.

Neutral molecule			Trication				
Energy [cm^{-1}]	Osc strength	Symm	Energy [cm^{-1}]	Osc strength	Symm		
1	12117	0.0	A'	1	6574	0.0	A'
2	24304	1.32	E'	2	21901	2.50	E'
3	26215	0.92	E'	3	23560	3.55	E'
4	29199	0.0	A'	4	29865	0.0	A'
5	30191	0.014	A''	5	30056	0.0	A'
6	30391	0.0	E''	6	31613	0.12	E'
7	30831	0.60	E'	7	32400	0.0	A'
8	31776	0.0	A'	8	33026	0.14	E'
9	33587	0.0	A'	9	34258	0.17	E'
10	34384	0.18	E'	10	34518	0.0	A'
11	36464	0.076	E'	11	36098	0.002	E'
12	36973	0.0	A'	12	39272	0.0	A'
13	37880	0.056	E'	13	39634	0.0	A'
14	38337	0.0	A'	14	39974	0.072	E'
15	41050	0.0	E''	15	40597	0.0	E''
16	41113	0.0035	A''	16	41453	0.0	A''
17	42336	0.25	E'	17	42081	0.012	E'

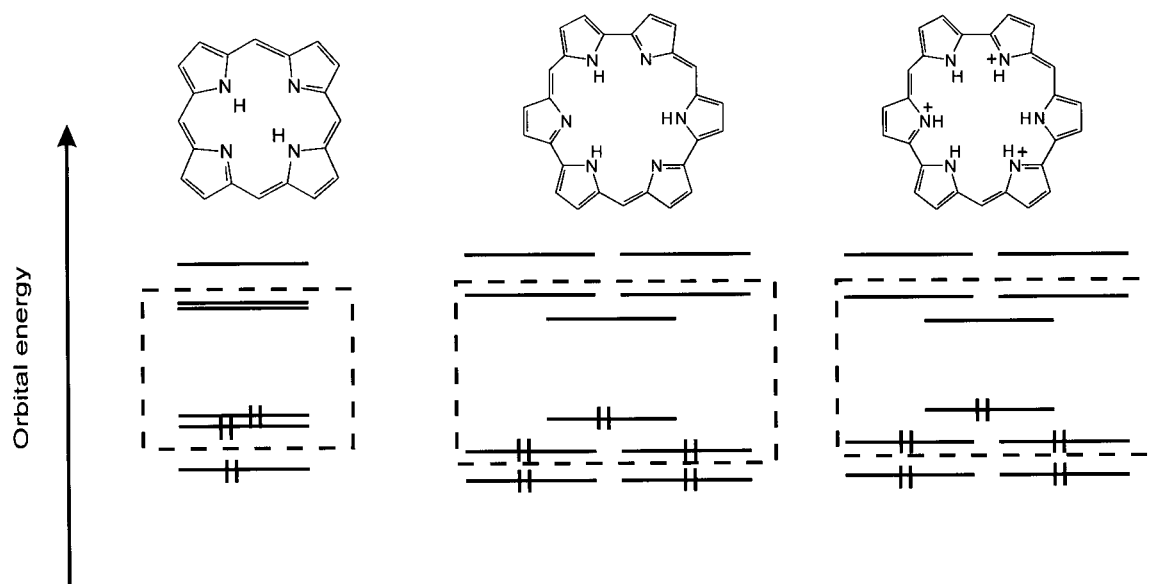


Figure 8. Energy ordering for the frontier orbitals in porphyrin, **1a** and **1b**. Dashed rectangles show the minimum basis set required for the description of lowest excited states.

the alkyl and phenyl substituents were replaced by hydrogen atoms. Excited-state calculations were then performed for these structures (Figure 9), which correspond to the distorted,

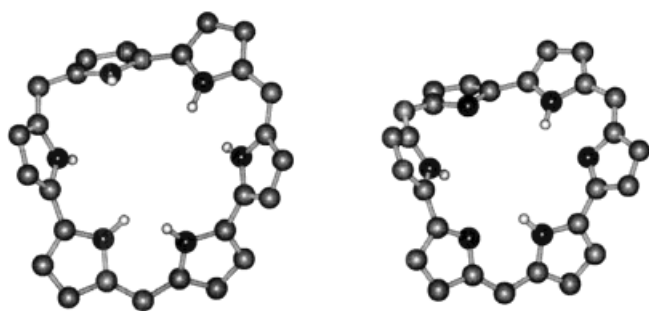


Figure 9. Geometry of the rosarin skeleton obtained after optimizing the structures **1a** (left) and **1b** (right) by molecular mechanics. These geometries were subsequently used for the excited state energy calculations.

parent rosarin. Such an approach has been shown to work for tetra-*n*-propyl-porphycene.^[21]

The results of calculations are presented in Table 3. Given the approximate character of the computational procedure, the agreement with experiment is surprisingly good. For both forms, the calculations predict a single weak transition in the low-energy region, well separated from the ensuing two strong ones at higher energy. The predicted energies of these transitions agree with experiment to about ± 1000 – 2000 cm^{-1} , well within the accuracy of the INDO/S method. The calculated and observed shifts between the fully protonated and the neutral form agree very well for both the strongest band and for the low-lying, weak one.

What seems most important is that the strongly distorted chromophore still “remembers” its symmetrical parentage. The calculated spectra for protonated and neutral forms are dominated by two strong, close-lying transitions in the visible

Table 3. Results of INDO/S calculations of transition energies and oscillator (Osc) strengths for the neutral and protonated forms of parent rosarin, strongly distorted from planarity.

Neutral molecule		Trication			
Energy [cm ⁻¹]	Osc strength	Energy [cm ⁻¹]	Osc strength		
1	15469	0.0016	1	11843	0.018
2	21787	2.64	2	19688	1.86
3	22410	1.24	3	19918	1.58
4	23552	0.12	4	22260	0.0046
5	24481	0.035	5	23240	0.013
6	24809	0.045	6	24850	0.077
7	26920	0.14	7	25882	0.0063
8	27559	0.069	8	27360	0.056
9	27765	0.12	9	28223	0.26
10	29587	0.013	10	28526	0.11
11	30273	0.033	11	28883	0.069
12	30603	0.14	12	29674	0.015
13	31151	0.25	13	30027	0.033
14	31542	0.027	14	30191	0.070
15	32246	0.011	15	30820	0.11
16	32244	0.027	16	30875	0.14
17	32514	0.028	17	32810	0.20
18	32724	0.21	18	33262	0.17
19	33141	0.004	19	33407	0.057
20	33568	0.022	20	33689	0.018

range, both in the planar and distorted structures. Only one transition, described mostly by a HOMO → LUMO configuration, is calculated to lie at lower energy than the two strong ones. Such a prediction stands in contrast to what is found for porphyrin. Here, the four-orbital, 2 × 2 CI basis model predicts two low-intensity Q bands, followed by two strong Soret transitions.

Conclusion

A combination of spectral and computational studies of various rosarin derivatives leads to the conclusion that the absorption pattern of this expanded porphyrin should differ from the typical sequence of Q and Soret bands observed for porphyrins. The main difference is the presence of only one transition in the low-energy region, due to the ordering of molecular orbitals. The minimal basis required for the understanding of the spectrum of rosarin consists of six orbitals, the three highest occupied and three lowest unoccupied ones. Nonetheless, it is remarkable that even a large distortion of the molecular skeleton from planarity exerts a rather small influence on the predicted spectral pattern.

The photophysics of the particular highly substituted rosarin (**1**) studied by experiment was found to be dominated by a rapid S₀ ← S₁ internal conversion, a process that occurs both at room and at low temperature. The fast rate of this process, most probably engendered by the nonplanarity of the system, precludes formation of the triplet state. Efficient population of the triplet state may, however, be achieved by exposing the system to an external heavy atom. In any event, a clear prediction from this work is that more planar rosarin

derivatives would be interesting to study. Such systems should show far less in the way of radiationless deactivation and should display longer lived and better populated excited singlet and triplet states.

Acknowledgment

This work was supported by the Polish Committee for Scientific Research (grants 3T09A 12108 and 3T09A 06314), by a grant from the Foundation for Polish Science ("Fastkin" program), and by the United States National Science Foundation (grant no. CHE-9725399).

- [1] a) "Expanded, Contracted and Isomeric porphyrins", J. L. Sessler, S. J. Weghorn, *Organic Chemistry Series, Vol. 15*, Pergamon, **1997**; b) J. L. Sessler, A. K. Burrell, *Topics Curr. Chem.* **1991**, *161*, 111; c) A. Jasat, D. Dolphin, *Chem. Rev.* **1997**, *97*, 2267.
- [2] a) A. Harriman, B. G. Maiya, T. Murai, G. Hemmi, J. L. Sessler, T. E. Mallouk, *J. Chem. Soc. Chem. Commun.* **1989**, 314; b) B. Henderson, T. J. Dougherty, *Photochem. Photobiol.* **1992**, *55*, 145; c) *Photodynamic Therapy: Basic Principles and Clinical Applications* (Eds.: B. Henderson, T. J. Dougherty), Marcel Dekker, New York, **1992**.
- [3] S. W. Young, F. Quing, A. Harriman, J. L. Sessler, W. C. Dow, T. D. Mody, G. Hemmi, Y. Hao, R. A. Miller, *Proc. Natl. Acad. Sci. USA* **1996**, *93*, 6610.
- [4] J. L. Sessler, S. Weghorn, V. Lynch, M. R. Johnson, *Angew. Chem.* **1994**, *106*, 1572; *Angew. Chem. Int. Ed. Engl.* **1994**, *33*, 1509.
- [5] a) S. Gentenmann, C. J. Medforth, T. P. Forsyth, D. J. Nurco, K. M. Smith, J. Fajer, D. Holten, *J. Am. Chem. Soc.* **1994**, *116*, 7363; b) S. Gentenmann, C. J. Medforth, T. Ema, N. Y. Nelson, K. M. Smith, J. Fajer, D. Holten, *Chem. Phys. Lett.* **1995**, *245*, 441; c) C. M. Drain, C. Kirmaier, C. J. Medforth, D. J. Nurco, K. M. Smith, D. Holten, *J. Phys. Chem.* **1996**, *100*, 11984; d) M. Ravikanth, T. K. Chandrasekhar, *J. Photochem. Photobiol. A: Chem.* **1993**, *74*, 181; e) M. O. Senge, *J. Photochem. Photobiol. B: Biol.* **1992**, *16*, 3.
- [6] J. L. Sessler, S. J. Weghorn, T. Morishima, M. Rosingana, V. Lynch, V. Lee, *J. Am. Chem. Soc.* **1992**, *114*, 8306.
- [7] J. Jasny, *J. Lumin.* **1978**, *17*, 149.
- [8] J. Dobkowski, Z. R. Grabowski, J. Jasny, Z. Zieliński, *Acta Phys. Pol. A* **1995**, *88*, 445.
- [9] J. Jasny, J. Sepioł, J. Karpiuk, J. Gilewski, *Rev. Sci. Instrum.* **1994**, *65*, 3646.
- [10] PCMODEL, Serena Software, Bloomington, IN.
- [11] N. L. Allinger, *J. Am. Chem. Soc.* **1977**, *99*, 4899.
- [12] M. J. S. Dewar, E. G. Zoeblich, E. F. Healy, J. J. P. Stewart, *J. Am. Chem. Soc.* **1985**, *107*, 3902.
- [13] J. J. P. Stewart, *J. Comput. Chem.* **1989**, *10*, 209, 221.
- [14] J. E. Ridley, M. Z. Zerner, *Theor. Chim. Acta* **1973**, *32*, 111.
- [15] S. J. Strickler, R. A. Berg, *J. Phys. Chem.* **1962**, *37*, 814.
- [16] B. Lament, E. Vogel, J. Waluk, unpublished results.
- [17] J. Dobkowski, V. Galievsky, A. Starukhin, E. Vogel, J. Waluk, *J. Phys. Chem. A*, **1988**, *102*, 4996.
- [18] a) P. Chmielewski, L. Latos-Grażyński, K. Rachlewicz, T. Głowiak, *Angew. Chem.* **1994**, *106*, 805; *Angew. Chem. Int. Ed. Engl.* **1994**, *33*, 779; b) H. Furuta, H. Asano, T. Ogawa, *J. Am. Chem. Soc.* **1994**, *116*, 767.
- [19] K. Rachlewicz, N. Sprutta, L. Latos-Grażyński, P. Chmielewski, L. Sztterenber, *J. Chem. Soc. Perkin Trans. 2*, **1998**, 959.
- [20] M. Gouterman, *J. Mol. Spectr.* **1961**, *6*, 138.
- [21] K. B. Andersen, E. Vogel, J. Waluk, *Chem. Phys. Lett.* **1997**, *271*, 341.

Received: February 5, 1999 [F1587]